Elucidation of The Roles of Metal Ions in Misfolding and Aggregation of TTRwt and TTR-V30M Associated with ATTR Amyloidosis

By

Kelley Burton

July 2024

Director of Thesis: Kwang Hun Lim

Major Department: Chemistry

Abstract

Misfolding and aggregation of transthyretin causes a range of diseases, many of which are caused by mutations and destabilization of the protein. Known diseases related to the protein include cardiomyopathy, polyneuropathy, and transthyretin amyloidosis, along with other ailments [1,2,3]. The mechanism by which these diseases and many others occur is currently unknown. Through previous studies, metals have been shown to induce aggregation of these proteins in which case it is hypothesized to have an impact on the mechanism's pathway [4,5]. Specifically, Zn^{2+} ions at significantly higher levels have been observed to induce ex-vivo TTR aggregates in patients affected by amyloidosis compared to those with no current signs of the disease[5]. The effectiveness of Ca^{2+} ions in triggering the neurodegenerative process linked to polyneuropathy is crucial in understanding the role of the metal [5]. Each of these metals has shown potential possibilities of their specific roles in interactions with transthyretin. Through this study, Zn^{2+} and Ca^{2+} ions were used throughout different experiments. WT TTR is a known native form of transthyretin that becomes unstable over time in the structural form[1]. This protein will be used in comparison with TTRv-V30M as it is one of the most common mutations with an

association with familial amyloid polyneuropathy (FAP)[3]. In this thesis, biophysical techniques such as aggregated kinetics, circular dichroism, and isothermal titration calorimetry were used to examine the effects of the metal ion binding. The aim of this study is to investigate the effects of the metal ions on the structure and dynamics of the protein associated with misfolding and aggregation. The biophysical analyses revealed the metal ion bindings induced local structural/ dynamical changes of the protein, promoting misfolding and aggregation.

Elucidation of The Roles of Metal Ions in Misfolding and Aggregation of TTRwt and TTRv-V30M Associated with ATTR Amyloidosis

A Thesis

Presented to the Faculty of the Department of Chemistry

East Carolina University

In Partial Fulfillment of the Requirements of the Degree

Master of Science in Chemistry

By

Kelley Burton

July 2024

Director of Thesis: Dr. Kwang Hun Lim, Ph.D.

Thesis Committee Members:

Dr. Anne M. Spuches, Ph.D.

Dr. Nathan E. Hudson, Ph.D.

Table of Contents

List of Figures

List of Abbreviations

Anion Exchange Chromatography……..…… AEC

Circular Dichroism…… CD

Cryogenic Electron Microscopy……. CRYO-EM

Familial Amyloidosis Cardiomyopathy…….…….... FAC

Familial Amyloidosis Polyneuropathy……...…… FAP

Fast Pass Liquid Chromatography……. FPLC

Hereditary Transthyretin Amyloidosis……... hATTR

Isothermal Titration Calorimetry……. ITC

Leucine 55 Proline Transthyretin…….……... L55P-TTR

Optical Density at 600 nm…….…… OD_{600}

Phosphate-Buffered Saline……. PBS

Rotations Per Minute……. RPM

Senile Systemic Amyloidosis……. SSA

Size Exclusion Chromatography..... SEC

Thyroxine……. . T4

Transthyretin…….. TTR

Transthyretin Amyloidosis…….……...……. ATTR

Valine 30 Methionine Transthyretin……..…… V30M-TTR

Valine 122 Isoleucine Transthyretin……..……. V122I-TTR

Wild -Type Transthyretin…….…… WT-TTR

Chapter 1

Introduction

1.1 Protein Folding and Misfolding

Proteins are one of the most complex substances that are found in all living organisms. They are essential to structural support, biochemical catalysts, hormones, enzymes, building blocks, and initiators of cellular death[6]. Each of these processes occurs in the human body and even though there are a multitude of different proteins, they are species-specific, and proteins differ from their specific duties in the human body[6]. It is important to understand from the multitude of different proteins that are being created and used throughout the body that they will not all be made to perfection[7]. When proteins are not produced to perfection, they are known as misfolded or defective proteins, which the body identifies through a quality-control mechanism[7]. Though most misfolded proteins are filtered out to be recycled back into the body, some of the misfolded proteins will bypass the quality-control mechanism. When misfolded proteins bypass the mechanism and enter the system as normal proteins, they typically gather in clumps of misfolded proteins and are a leading cause of human degenerative diseases[7]. These misfolded proteins create non-native species, which will deposit themselves around the body and cause detrimental effects to the protein's native location. As these non-native species are created, they can form amorphous aggregates, oligomers, and amyloid fibrils [3,8,9].

1.2 Amyloids and Amyloidosis

Amyloids are a product of misfolded proteins that are formed from various peptides and proteins with diverse primary, secondary, and tertiary structures during their folded states[10]. These structures are predominantly β-pleated sheets aligned with an antiparallel structure that is

typically found in dense tissue deposits throughout the body. They are generally stable and insoluble in the native form in the presence of an aqueous buffer though they are not easily recognizable to the body and become foreign substances introduced to the immune system [8,10]. These amyloids can be acquired in such places as the liver, spleen, kidney, heart, nerves, and blood vessels[10,11,12]. The formation of amyloids and buildup in a specific location of the body with aggregation will formulate cytotoxic oligomers, and protofibrils and eventually develop amyloid fibrils [8,12]. The continued build-up of these proteins will cause diseases such as amyloidosis.

Amyloidosis is characterized by being developed from the deposits of elongated, unbranched protein fibrils on soft tissues and organs throughout the body. The amyloid fibrils that are associated with the individual can be hereditary or acquired through a natural process[12]. These protofibrils and amyloid fibrils can be deposited both locally and/ or systemically to the individuals. There are currently 60 known precursor proteins that are confirmed to be associated with amyloid protein fibrils. There are currently 27 proteins that are directly related to known human diseases[13]. With many unknown factors and determinations to an individual's diagnosis, it is imperative for the detection of the disease as it will allow for treatment if identified earlier on.

Hereditary (ATTR) Amyloidosis is known to have several different types. This form is caused by autosomal-dominant mutations, which accelerate the dissociation of the native protein transthyretin and pathological disease progression[12,14]. The most common is ATTR amyloidosis in which protein deposits cause severe peripheral and autonomic neuropathy and cardiac or renal disease[13,15,16]. This disease can cause death within 5 to 15 years of system onset when undiagnosed[15]. Typically signs and symptoms of ATTR amyloidosis include hyperesthesia to pain and temperature, motor weakness, decreased bowel motility, weight loss, and continued and

diminished deep-tendon reflexes to name a few[15]. This disease has been linked to three main conditions such as senile systemic amyloidosis (SSA), familial amyloidosis cardiomyopathy (FAC), and familial amyloidosis polyneuropathy (FAP)[1,16]. Senile systemic amyloidosis (SSA) is a form of amyloidosis that is associated with aging. The typical age of an individual to be diagnosed with SSA is over the age of 80 though in undiagnosed cases the age of an individual to have it could be much younger such as the age of 50[1]. The cause of this disease is amyloids being deposited in the myocardium, which results in arrhythmia and/ or heart failure. Familial amyloidosis cardiomyopathy (FAC) is a form of amyloidosis that is caused by mutated amyloids that have been aggregated and deposited into the myocardium. This type of amyloidosis tends to cluster into geographic and/ or ethnic groupings that exhibit autosomal dominant patterns of inheritance [13,15,17]. As inheritance plays a critical role in having this disease, age still plays a factor in when the disease symptoms will begin and the date on which the diagnosis would be determined is a factor in what treatments are possible. Familial amyloid polyneuropathy (FAP) is also an autosomal-dominant disorder that is due to mutations of transthyretin. This disease has symptoms of loss of peripheral sensory and autonomic polyneuropathy starting in the feet, loss of temperature sensation along loss of pain sensation [16,18]. FAP can affect the heart and kidney if the mutated protein causes build-up and loss of function in the affected areas. FAP is dependent on the age, origin, and mutation of the protein [19]. When the disease is diagnosed it raises the question of what the possible treatments are, which is dependent on how early the disease was detected. Each of these amyloid-related diseases is affected by the same protein, which is Transthyretin.

1.3 Transthyretin

Transthyretin is a 127-amino-acid β-sheet-rich tetrameric protein typically secreted into the blood through synthetization[1]. The protein is produced locally by the choroid plexus and by the retinal pigment epithelial cells and it is then secreted into the cerebrospinal fluid and eyes. The main purpose behind the protein is to transport the hormone thyroxine (T4) to plasma and cerebrospinal fluid [1,2]. The concentration of transthyretin in the blood is known to be between 20-40mg/dL and the concentration in cerebrospinal fluid is between 1.5-2.5 mg/dL [20,21,22,23]. The overall structure of transthyretin is shown below in Figures 1.1 and 1.2, it is seen that transthyretin is developed by two funnel-shaped T4-binding sites, with two of the T4-binding sites that are identically located at the dimer-dimer interface. Each of the dimers is then made from two monomers. The monomers are produced from eight β-strand chains and an α-helix motif, which forms the two four-β-stranded antiparallel sheets, along with several random coils [24,25]. Even though the β-sheet rich features are seen on the TTR monomers, these are the only forms of the TTR that are known to cause misfolds and mutations of the protein.

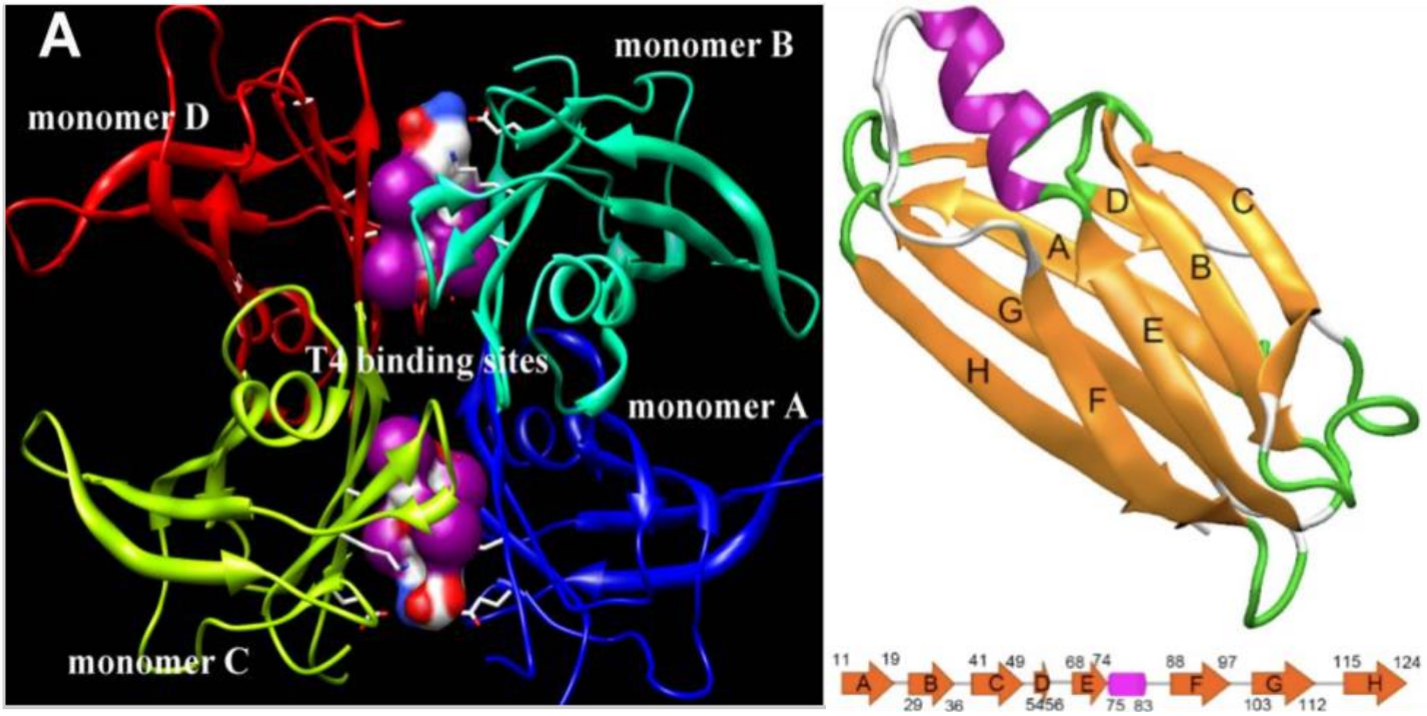

Figures 1.1 and 1.2: Model breakdowns of Transthyretin. Figure 1.1 shows the initial breakdown with the 4 monomers that bind to create Transthyretin [24]. Figure 1.2 is a monomer of transthyretin comprised of the two four- β-stranded antiparallel sheets [25].

Through the process of transporting hormones, the protein will dissociate into monomers and misfold rapidly and this is the cause of the build-up of amyloid fibrils. It is shown below in Figure 1.3 [3]. As the protein continues to have misfolding occur during production and the mechanism does not detect and destroy the mutated protein it causes a build-up of protein which in turn causes transthyretin amyloidosis. These are a set of systemic diseases that are commonly associated with some known and unknown aggregation along with extracellular depositions seen in deep tissues[3].

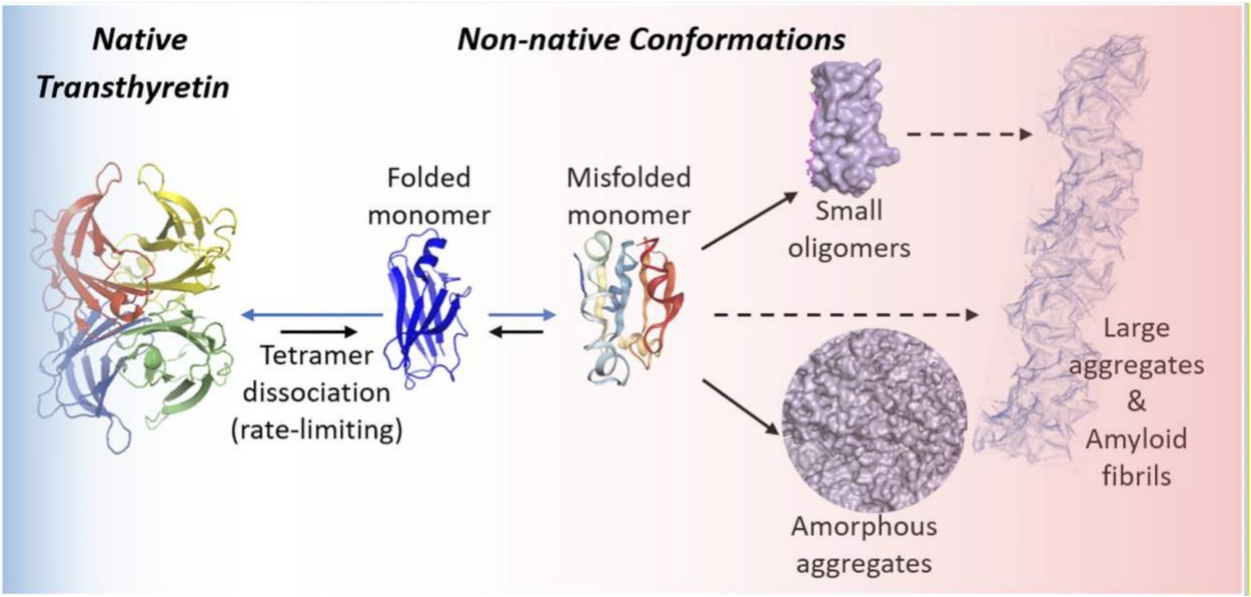

Figure 1.3: Non-native conformation mechanism of transthyretin and the breakdown of how the small oligomers and amorphous aggregates that form from the misfolded protein will lead to the build-up of large aggregates and amyloid fibrils[3].

One of the most commonly known mutations associated with this disease is Valine 30 Methionine (V30M), which is associated with the disease known as familial amyloid polyneuropathy (FAP). This disease is life-threaten that is caused by the accumulation of the amyloidogenic transthyretin protein. This disease alone affects 15,000-50,000 individuals worldwide and the life expectancy of an undiagnosed individual with this form of mutation is 10 to 12 years of age [19]. Another mutation of transthyretin is known as Wild-type ATTR Amyloidosis (WT), which is an age-related disease that is not caused by any known genetic mutations. This form is known to affect individuals at an older age, which causes their transthyretin protein to become less effective and less stable with the progression of their age. The amyloid fibrils developed from the mutation are typically developed and deposited in the heart[26,27]. This in turn can lead to Familial Amyloid Cardiomyopathy (FAC) as it is commonly

seen in adults over the age of 60 [13,15,17]. Mutations and diseases caused by transthyretin such as these are still relatively unknown as pinpointing and correcting these issues are still being researched for further discovery. There are currently treatments to yield the progression of amyloidosis though there is no current cure known. Treatments available for FAP, V30M specific is liver transplantation, which allows for first-hand suppression of the main source of the mutant. In severe cases, there have been times when they have suggested kidney-liver or heart-liver transplantation[1]. A medication has also been suggested in the early onset of the disease it is called tafamidis and it is used as a specific stabilizer of TTR. Tafamidis helps slow the progression of peripheral neuropathy in patients. There are other current investigative treatments and research being conducted to help improve an individual quality of life though there are still many unknown factors to these diseases and how the misfolding of transthyretin occurs [1,4,17].

Through research being conducted it has been a relatively new determination to look at what an individual body can handle in treatments versus what their body cannot handle. In many cases, acidic conditions have been observed to see if higher acidic conditions would induce aggregation of mutations. As testing continued it became more prominent to look at the physiological pH of the body as it may have a significant difference in comparison to the induced aggregation of the proteins[23]. Some notable metals that have shown induced aggregation with transthyretin mutated proteins include Zn^{2+} and Ca^{2+} ions, this is just the beginning of possibilities of how metals could induce aggregation of proteins.

1.4 Transthyretin and Metal Binding

Metal ions have played different roles and affect protein conformations differently. Transthyretin under certain conditions such will cause the protein to dissociate into partially

unfolded monomers that aggregate and form amyloidogenic fibrils. Metals ions such as Zn^{2+}, Cu^{2+}, Fe^{2+}, Mn^{2+}, and Ca^{2+} play a critical role in transthyretin amyloidogenic pathways. The use of each metal ion plays a different role and through research metals such as Cu^{2+} and Fe^{2+} ions showed unusual conformational changes. While Mn^{2+} ions showed very little difference in the structure[5]. In several studies, Zn^{2+} ions have been shown to bind to the transthyretin protein both in vitro and in vivo. It also shows higher levels of the ions inducing the formation of the amyloids being deposited in vitro. This began the hypothesizing of the possibility of Zn^{2+} ions binding onto the transthyretin protein that would possibly induce structural changes, triggering the amyloido-genesis process. Ca^{2+} ions are another metal that has been involved in the regulation of cellular signaling pathways and tissue homeostasis. In several studies, Ca^{2+} ions have been shown to be a key factor in the triggering of neurodegenerative processes. These studies also showed that an increase in metal present increases the rate at which fibril formation in transthyretin occurs. This suggests that Ca^{2+} ions dysregulation may have a role in the onset of transthyretin amyloidosis [5,28].

Zn^{2+} and Ca^{2+} ions have shown significant effects in general studies of the effective roles they have when induced with the transthyretin protein. Each of these metals was selected in the research to find the overall effectiveness they have when introduced to the proteins. The metal Zn^{2+} was found predominately with elevated concentration as the metal is present in the human body. The concentration of Zn^{2+} in the blood ranges from 12-18 μmol/ L and in the cerebral spinal fluid having a range of 0.5-3.0 μmol/L [23,28]. This allows for specific concentration targeting of the metal and the effect it has with transthyretin at physiological pH. It has also been theorized that Zn^{2+} has a low binding affinity to this protein. Though there have been binding sites located on the transthyretin structure. Currently, there are 16 binding sites with 12 binding

sites that have been determined [28]. The figure below shows the binding sites currently known with Zn^{2+} binding to transthyretin.

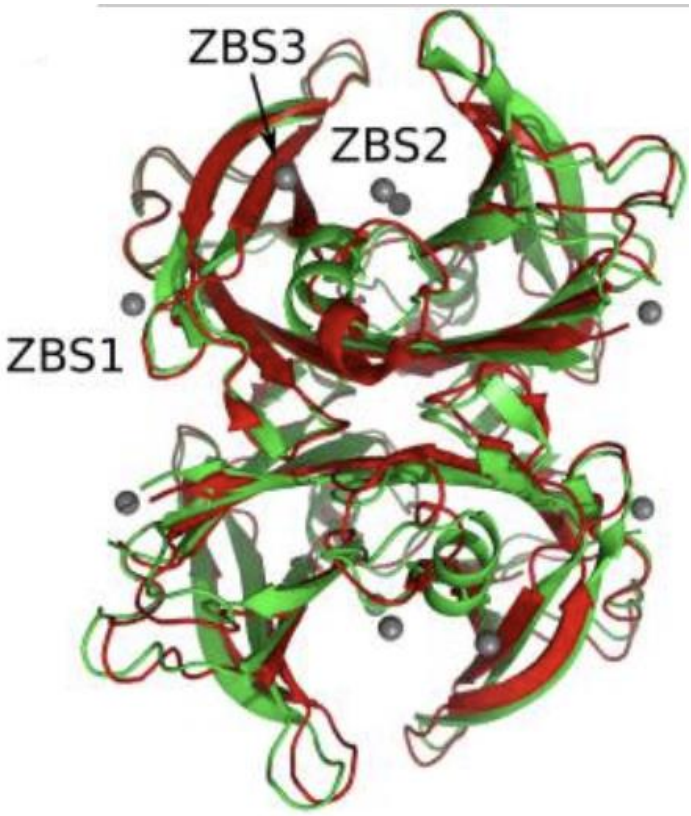

Figure 1.4: The binding sites of Zn^{2+} ions. They are pinpointed throughout the transthyretin protein by the grey dots. There are currently 12 known binding sites [28].

The metal Ca^{2+} has shown to be effective in triggering the neurodegenerative process that is associated with polyneuropathy which is significant in how the metal plays a role throughout the process. Ca^{2+} is another naturally occurring metal in the body with concentration in the blood having a range of 1.2-1.4 mmol/L and in the cerebral spinal fluid having a range of 2.0-4.0 mmol/L [29]. This also allows for specific concentration targeting of the metal and its effects with binds to transthyretin at physiological pH. With the presence of the metal in the body and is found commonly in areas where the protein is present it allows for a moderate binding affinity[30].

Below in Figure 1.5 is an example of two of the binding sites that have been identified with a total of six being found.

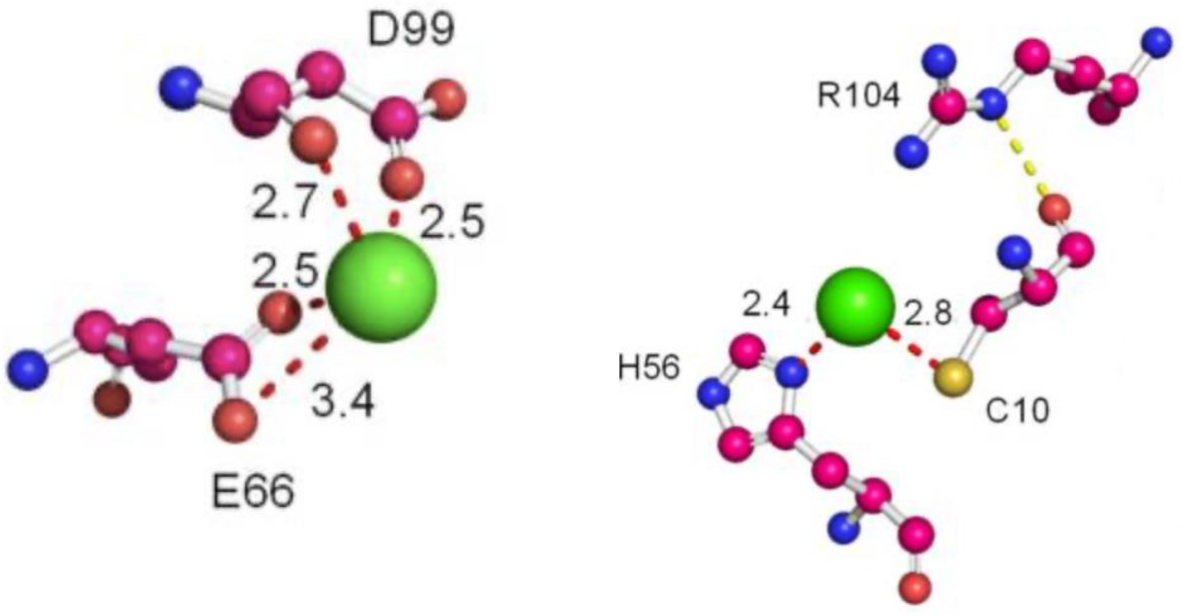

Figure 1.5: Shows the known binding sites of Ca^{2+} ions. The binding site is formed by the backbone of carbonyl, the carboxylic group and a water molecule not shown [29].

These metals will be used throughout different experiments and future experiments to identify the effectiveness they have and induce aggregation of the protein. Experiments that include both Zn^{2+} and Ca^{2+} ions include aggregation kinetics, Circular Dichroism, and Isothermal Titration Calorimetry. Each will play a role in identifying the effectiveness of the metals in binding to the protein and inducing aggregation.

1.5 Research Objective

Molecular mechanisms of the structural transition of the natively folded protein to amyloids are not currently understood. It is hypothesized that its structural change occurs during the transitions from the native folded to the unfolded (full or partial) intermediate states showing the possibility of mutations such as conformational transitions, accelerating in misfolding and aggregation [31,32]. With little understanding of how these mutations occur with transthyretin, early testing has been conducted with the use of metal ions as they have been known as possible causes of inducing protein aggregation, which produces amyloid fibrils. Two specific metal ions such as Zn^{2+} and Ca^{2+} have been shown to induce and accelerate the aggregation process both in vivo and ex vivo [5].

The use of both metal ions and early results of induced aggregation is a stepping stone in understanding how these metal ions affect transthyretin. The focus will be to observe the effects of the metal ions and their role during the structural transition of the native protein. The next step will be observing how the metal ions will affect the aggregation kinetics of specific mutates of the native protein form. The data will then be compared by the molecular structures of the mutates and the native transthyretin.

Along with aggregation kinetics, metal ions may introduce changes to the native form both conformational and dynamical changes that induce the structural transition to aggregation-prone states. To observe these changes the use of ITC will be used to observe both enthalpy and entropy changes to the metal ions bindings. CD will also be used to observe the secondary structure of the native and mutated forms to see if any significant changes are observed. Therefore, each of these specific methods will show initial insight into how specific metal ions affect transthyretin's native and mutated form.

Chapter 2

Protein Preparation

2.1 Transformation and Expression

In preparation for protein transformation and expression, the initial step was to prepare LB stock and media. The LB stock solution was prepared using LB Broth (Miller)(5.00 g) and dissolved into deionized water (200 mL). The media was prepared in three Fernbach flasks (2.8 L), each containing LB broth (Miller) (25 g) and deionized water (1 L). The media Fernbach flasks and the stock solution were all autoclaved on a liquid cycle (20 mins, 121°C). All solutions are cooled prior to use.

Once solutions were prepared and cooled a carbenicillin plate (1g/10mL, filtered through 0.22µm filter paper) was removed from the refrigerator and placed into an incubator (37°C). The desired plasmid (-20 °C, Isotemp, Refrigerator/Freezer, Fisher Scientific) and E. coli strain BL21(DE3) (-80 °C, Isotemp, Fisher Scientific) were removed from their perspective freezers and placed on ice. E. coli (20 µL) was pipetted into a culture tube and marked as used. The plasmid (1 µL) was then directly pipetted onto the E. coli in the culture tube. The mixture was then placed on ice (2 mins). After cooling it was placed into a hot water bath (42°C, 1 min) and then placed back onto ice (2 mins). After the temperature shock, stock LB broth (80 µL) was pipetted into the culture tube and shaken in an incubator (1 hr., 250 rpm, 37°C). The sample (50 µL) was pipetted and spread on the preheated (37°C) carbenicillin plate with the use of a sterilized iron spreader (20% ethanol and Bunsen burner). The plate was incubated agar side up without shaking (15 min, 37°C). The plate was flipped to agar side down and allowed to incubate without shaking (12-14 hours, 37°C).

The plate was removed from the incubator, and it was ensured to be suitable growth. Six culture tubes were collected as for every 500 mL of LB equals one culture tube. For each tube stock, LB (5 mL) broth and ampicillin (5 µL) were placed into each tube and a sterilized colony scraper containing a larger colony was dipped into a culture tube for each of the six culture tubes. The culture tubes were placed into an incubator until the solution became turbid (3-4 hours, 37°C, 250 rpm). Once the tubes were turbid, ampicillin (1 ml) was added to each of the Fernbach flasks containing the LB broth (1 L). The culture tubes were transferred into the Fernbach flask (two culture tubes per 1L of LB broth). The flasks were incubated (1 hour, 37°C, 250 rpm) and the OD_{600} was observed with the use of the UV-Vis Spectrophotometer (600 nm). Once the reading met the absorbance range of (0.6-0.8) an addition of IPTG (500 µL, 1M solution) was added into the flask and allowed to incubate and shake overnight (25°C, 250 rpm).

The next morning the OD_{600} was observed until it read over 1.5. Once the OD was met the solution was centrifuged (Sorvall Legend XTR Centrifuge, Thermo Scientific)(8000 rpm, 30 mins) into centrifuge bottles (3 bottles containing ⅔ of the sample). The supernatant was discarded into a waste flask and this process was continued until all samples had been centrifuged. The protein was stored in a deep freezer (-81°C) until purification of the protein was needed.

2.2 Purification

In preparation for protein purification, the initiation step was to thaw the protein pellets from the deep freezer (-81°C)(30 minutes). Once thawed the protein pellets were then mixed with lysis buffer ((20mM Tris, 150mM NaCl), 50mL per Liter of LB). The mixture was then placed in a chilled metal beaker on ice. Sonication was then performed by placing the spout

halfway from the bottom of the chilled metal beaker containing the mixture and pressing the start button on the (Sonic Dismemberator Model 505, Fisher Scientific). The sonication settings were set at 50% amplitude with pulsing for one minute with one-minute rest periods (completed five times). The sample was then evenly distributed between two centrifuge tubes and centrifuged (8000 rpm, 30 mins). Once centrifuging was completed the protein supernatant was placed into another chilled beaker (400mL), and ammonium sulfate (50% saturation) was added to the protein supernatant and then allowed to stir (15 minutes). After the addition of ammonium sulfate, the supernatant was placed evenly into two clean centrifuge tubes and centrifuged once again (8000 rpm, 30 mins). Next, the protein supernatant was placed into prepared dialysis bags which were cut to allow for 40-50 mL of sample in each and they were hydrated with the use of deionized water (15 mins). Once the supernatant was evenly placed into the dialysis bags, they were placed into a chilled two-liter dialysis buffer (12.5 mM Tris buffer, 0.5 nM EDTA, and PMSF) overnight while stirring. The buffer was exchanged with a new chilled dialysis buffer the next morning. It was allowed to stir again overnight.

The denatured protein was collected from the dialysis bags and then was filtered through a 0.45µm filter paper with a filter apparatus which was connected to a house vacuum. The filtered sample was then placed into a chilled beaker until the Atka pure FPLC instrument and column (10 mL HiTrap^{TM} Q HP (GE Healthcare) AEC) was prepared for an anion exchange. The instrument was cleaned with ethanol (20%) and then washed with buffer A (20 mM Tris buffer pH 8, 2 mM EDTA pH 8.0) for 30 minutes with parameters of 2.000 mL/ min, 30.000 mL volume. The protein was then eluted into a factional collector using the Q_10mL_rev method. This method included washes (four) using a gradient increase (5%) in Buffer B (20mM Tris, 5M NaCl, pH 8.0) flowthrough. Buffer B was then used to gradually increase the amount in the

column to elute the protein into the fractionation collector. Once the method was completed the highest concentrated fractions (2 mL each) were collected into a beaker and then saturated with ammonium sulfate (90%) for 15 minutes. This allows for the protein to be pulled from the solution and absorbed into the ammonium sulfate. The cells are pure protein; most if not all of the impurities were removed with the supernatant. After the addition of ammonium sulfate, they were centrifuged down to cells with the microcentrifuge and stored at 4°C.

The samples were removed from the 4°C freezer resuspended in the supernatant (1.00mL) and spun in microcentrifuge tubes (Sorvall Legend Micro 17 Centrifuge, Thermo Scientific, 10 minutes at 10k rpm). The supernatant was removed, and the pellets were dissolved in deionized water (2.00 mL). They were microcentrifuge again with the same initial parameter. The samples were prepared for size exclusion. The FPLC instrument with the size exclusion column (HiLoad© 16/60 Superdex 200 gel SEC) attached was washed with 10mM phosphate buffer (2.6mM monobasic stock, 4mM dibasic stock, 100 mM KCl, and 1mM EDTA) with a pH of 7.4 at a flow rate of 1.000mL/ min for 120.00 min. After the washing and conditioning of the column, the system was set to a flow rate of 1.000 mL/ min at 120 mins with fractionation collection (2.00 mL). The system injector was washed with deionized water (3 times); the protein sample was then injected into the instrument, Once the method was completed the highest concentrated fractions were collected, and stored at -81°C.

2.3 Desalting and Buffer Exchange

In preparation for buffer exchange, the protein fractions necessary for future experiments were removed from the freezer (-80 °C, Isotemp, Fisher Scientific) and thawed. The FPLC with a desalting column was used for a buffer exchange of the protein into a Bistris solution. The FPLC

instrument with the desalting column (HiTrap™ Desalting 5mi) attached was washed with Bistris buffer (25 mM BisTris, 50 mM NaCl) with a flow rate of 2.000mL/ min for 30.00mL. After the washing and conditioning of the column, the system was set to a flow rate of 2.000 mL/ min for 30.00 mL with fractionation collection (1.00 mL). The system injector was washed with deionized water (3 times); the protein sample (1.50 mL) was then injected into the instrument. The highest concentrated fractions were then collected and used for experimentation or stored at 4°C until further use.

Chapter 3

Experimentation

3.1 Aggregation Kinetics

Once the desalting and buffer exchange were completed the highest concentrated fractions were collected and the concentration was determined with the use of the UV-Spectrophotometer (280 nm, Evolution 201 UV- Visible Spectrophotometer). The information collected from the UV-Spectrophotometer was then used in a series of calculations and with the use of the extinction coefficient ($7.76 \times 10^4\ M^{-1}\ cm^{-1}$)[33] to determine each solution volume needed for sample preparation. Below is an example calculation of the determination of a protein concentration to vary between 0.25 mg/ mL to 0.5 mg/ mL (mg/mL= g/L).

$$0.5\ g/L \times 1000\ \mu mol/\ 13.8\ g = 36.\ 23\ \mu mol/L = 36.23\ \mu M \quad \text{(Equation 1)}$$

The next step was then to determine the amount of metal solutions needed for each condition. The metal solutions used for aggregation kinetics included Zn^{2+} (25 mM Bistris, 50 mM NaCl, 25 mM Zn) and Ca^{2+} (25 mM Bistris, 50 mM NaCl, 50 mM Ca) each made to have a concentration to vary between 0.1 mg/ mL to 0.75 mg/ mL. To determine the amount of metal solution needed for aggregated kinetics is shown below in an example calculation (equation 2).

$$\text{Volume (uL)} = 36.23\ \mu M\ \text{Protein} \times 5 \mu M\ \text{Metal}/\ 1\ \mu M\ \text{Protein} \times 1 mL/\ 100 mM\ \text{Metal} \quad \text{(Equation 2)}$$

$$= 1.81\ \mu L_{Metal}$$

Once the metal volume needed for the experiment was determined the necessary volume of the protein was then determined based on equation 3.

$$1000\ \mu L\ \text{solution} = Vol_{protein} + Vol_{metal}$$

$$1000\ \mu L\ \text{solution} - Vol_{metal} = Vol_{protein} \qquad \text{(Equation 3)}$$

$$1000\ \mu L\ \text{solution} - 1.81\ \mu L_{metal} = Vol_{protein} = 998.19\ \mu L_{protein}$$

After the determination of volumes needed for both protein and metals the determined volumes were then placed into the prelabeled cuvettes. The cuvettes were caped and parafilm was then placed on each capped cuvette to ensure complete closure of the cuvettes. Each sample was also prepared in duplicate to observe calculation errors and variability in the preparation of the samples.

The initial absorbances were collected on the UV-visible spectrophotometer and data was then entered into appropriate spreadsheets. The subsequent readings were then recorded every 30 minutes, 45 minutes, and 1 hour throughout 4 to 10 hours. During the interim times, the samples were placed in a styrofoam holder properly labeled and placed into a benchtop incubator/shaker (Excella E25 Incubator Shaker) (250 rpm, 37°C). The data collected during this experiment were treated as a measure of aggregation. As the absorbance values became higher during data collection, it showed that there was a higher measurement of aggregation in the samples. As the samples reached an absorbance of 0.200 it showed turbidity and over time when the absorbances continued to climb, the higher the turbidity of the sample. Once aggregation kinetics was completed and all data had been collected the samples were then combined in microcentrifuge

tubes and microcentrifuge (10 minutes, 10k rpm) to condense for the collection of cells. They were then stored in the refrigerator (4°C) until further testing.

3.2 Circular Dichroism

Once the desalting and buffer exchange were completed the highest concentrated fractions were collected and the concentration was determined with the use of the UV-Spectrophotometer (280 nm, Evolution 201 UV- Visible Spectrophotometer). The information collected from the UV-Spectrophotometer is then used in example equations 1-3 to determine each concentration solution volume needed for sample preparation. The concentration needed for CD was 1 mg/mL. The initial native stated was diluted with buffer (1 mg/mL, 25 mM BisTris, 50 mM NaCl). The Zn-induced aggregate required to have at least 2 mL of ~2.5 mg/mL stock. The final metal: protein ratio should be ~1:200 (25 mM Bistris, 50 mM NaCl, 25 mM Zn). The Ca-induced aggregate required to have at least 2 mL of ~2.5 mg/mL stock (25 mM Bistris, 50 mM NaCl, 50 mM Ca) with a final metal: protein ratio of ~1:400. The Zn and Ca-induced aggregate solutions were then incubated (4 hours -up to a week). The native solution is then placed in a refrigerated (4°C) until use. After incubation, the metal-induced aggregates were then centrifuged (10 minutes, 10k rpm) to remove precipitates. The native and metal-induced aggregates were then resuspended in ~100μL of buffer solution (25 mM BisTris, 50 mM NaCl) to observe the concentrations. Guanidine HCl (3.5 M) was then used along with the samples to check concentrations. The solutions were diluted with buffer (1 mg/mL, 25 mM BisTris, 50 mM NaCl) and then diluted each solution with deionized water to bring the protein and buffer concentration down to the necessary concentration for the experiment (0.2 mg/mL, 5 mM BT, 10 mM NaCl).

The Circular Dichroism system setup included opening the value of the nitrogen gas tank to purge oxygen from the system. The water bath and temperature controllers were then switched on. The spectrometer was then turned on and a wait time of 30 minutes was needed before turning on the lamp of the system. Once the lamp was initiated, another 30-minute waiting period was needed for the lamp to warm. The next step was to open the Spectra Manager system on the computer select the spectrum measurements under spectra analysis and load in the experiment parameters (6 scans per sample, 50nm per min). Buffer solution (~300 µL, 5 mM BT, 10 mM NaCl) was pipetted into the cuvette and the cuvette was then placed into the CD chamber and the run sample button was then clicked. Each sample was run in this same manner. After each spectrum was collected and automatically saved into the system, they were renamed to their appropriate name correlating to each sample. The values were then exported via CSV for use in an Excel spreadsheet. The data was then analyzed for the results of the samples.

3.3 Isothermal Titration Calorimetry

3.3.1 Nano Isothermal Titration Calorimetry

Once the desalting and buffer exchange were completed the highest concentrated fractions were collected and the concentration was determined with the use of the UV-Spectrophotometer (280 nm, Evolution 201 UV- Visible Spectrophotometer). The information collected from the UV-Spectrophotometer was then used in example equations 1-3 to determine each concentration solution volume needed for sample preparation. The protein concentration needed for ITC was 0.20 mM and the dilution needed was calculated for the protein and the sample was prepared. Along with the protein sample prep, the metal (25 mM Bistris, 50 mM NaCl, 0.25 mM Zn) solution needed for the experiment was also prepared. The Nano ITC LV

was first calibrated, and the method needed was placed into the system setup. The system setup included an incremental titration with 24 injections, with injection intervals (200 s) and data intervals to be set at one. The injection volume was set to be 2.02 μL. The expected heat was to be medium with a temperature set point (25°C). The syringe volume was set to 50 μL and the system had a stirring rate of 350 RPMs.

Once the method was set the cover was removed from the system and large forceps were used to remove the reference needle from the reference cell. The reference cell was cleaned three to four times with purified water. After rinsing, purified water (300 μL) was placed back into the reference cell and the needle was placed back into the reference cell with forceps. The sample cell was also rinsed with purified water (three to four times, 300 μL). The sample syringe was also rinsed with purified water (1000 μL) to ensure all tools and the system were clean. The micropipette was then used to place the metal (25 mM Bistris, 50 mM NaCl, 0.25 mM Zn, 50 μL) into the syringe horizontally. The plunger was then placed into the syringe gently to ensure little to no air would be introduced into the syringe. The cover was then inverted, and the syringe was then placed invertedly to screw into the cover. The sample cell was filled with the protein (300 μL, 20 mM). The cover and syringe were then turned back to a vertical position and placed into the column in the locked position. The start mix button was pressed and then the overall start button was pressed. It is typically seen to have an equilibration time of 600 seconds for the start and ending of the experiment. Once the experiment was completed the raw data was collected to then determine the corrected data with NanoAnalyze.

3.3.2 MicroCal Isothermal Titration Calorimetry

Once the desalting and buffer exchange were completed the highest concentrated fractions were collected and the concentration was determined with the use of the UV-

Spectrophotometer (280 nm, Evolution 201 UV- Visible Spectrophotometer). The information collected from the UV-Spectrophotometer was then used in example equations 1-3 to determine each concentration solution volume needed for sample preparation. The protein concentration needed for ITC was 0.24 mM and the dilution needed was calculated for the protein and the sample was prepared. The metal (25 mM Bistris, 50 mM NaCl, 0.25 mM Zn) needed for the experiment was also prepared. The MicroCal VP-ITC was first calibrated, and the method needed was placed into the system setup. The system setup included an incremental titration with 29 injections, with injection intervals (120 s) and data intervals to be set at one. The injection volume was set to be 2.00 μL for the first injection and then all subsequent volumes were set to 8.00 μL. The expected heat was to be medium with a temperature set point (25°C). The syringe volume was set to 240 μL and the system had a stirring rate of 307 RPMs.

Once the method was set the cover was removed from the system and large forceps were used to remove the reference needle from the reference cell. The reference cell was cleaned three to four times with purified water. After rinsing, purified water (240 μL) was placed back into the reference cell and the needle was placed back into the reference cell with forceps. The sample cell was also rinsed with purified water (three to four times, 240μL). The sample syringe was rinsed with purified water (1000 μL) to ensure all tools and the system were clean. The syringe was then placed into the metal (25 mM Bistris, 50 mM NaCl, 0.25 mM Zn) and it was sipped into the syringe to the necessary volume needed (240μL). The sample cell was filled with the protein (1.8 mL, 0.20 mM, 1.4mL) per pipet. The cover and syringe were then placed into the column in the locked position. The start mix button was pressed and then the overall start button was pressed. It is typically seen to have an equilibration time of 600 seconds for the start and

ending of the experiment. Once the experiment was completed the raw data was collected to then determine the corrected data with NanoAnalyze.

Chapter 4

Results

4.1 Aggregated Kinetics

4.1.1 Preliminary Results

Aggregation Kinetics data was initially collected and placed into a spreadsheet to observe the changes in absorbance over a period of time at physiological pH as these conditions are stable in the human body. These initial results show how different amount of metal affects the protein aggregation properties in a period of 4 to 6 hours. Figures 4.1 and 4.2 show the correlation of how different variations of Ca^{2+} introduced into V30M and WT affect protein aggregation. As shown the amount of metal used in each sample shows a consistent aggregation correlation pattern over a period of time. These graphs show that V30M is a more reactive mutation than WT with the metal ions present.

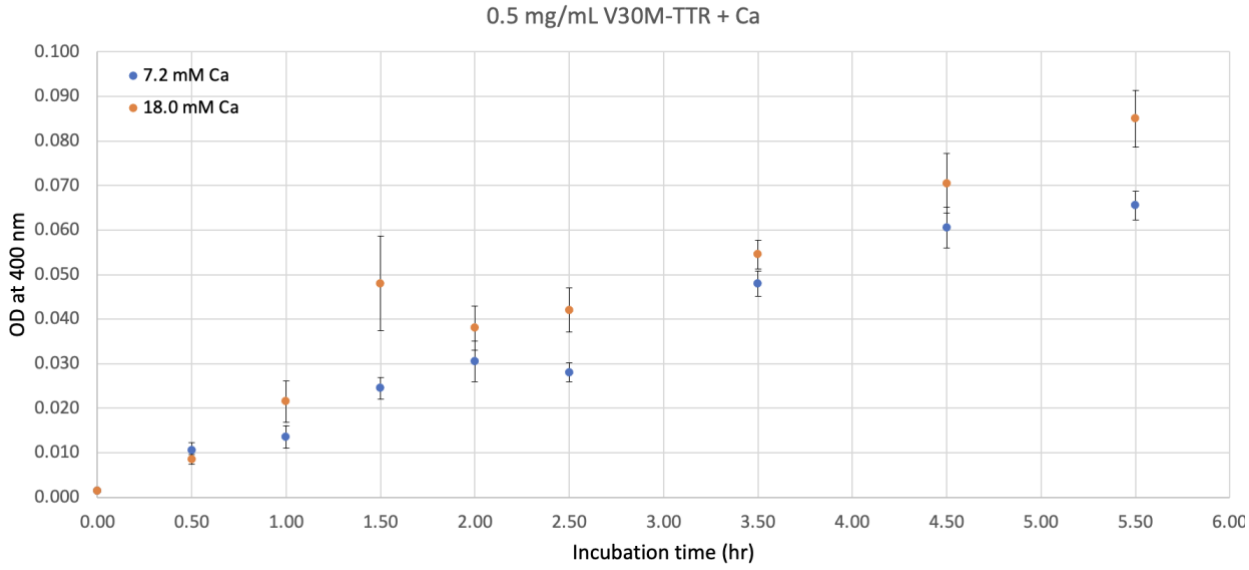

Figure 4.1: Preliminary data of 0.5mg/ mL V30M-TTR + Ca with concentrations of 7.2 mM and 18.0 mM of Calcium.

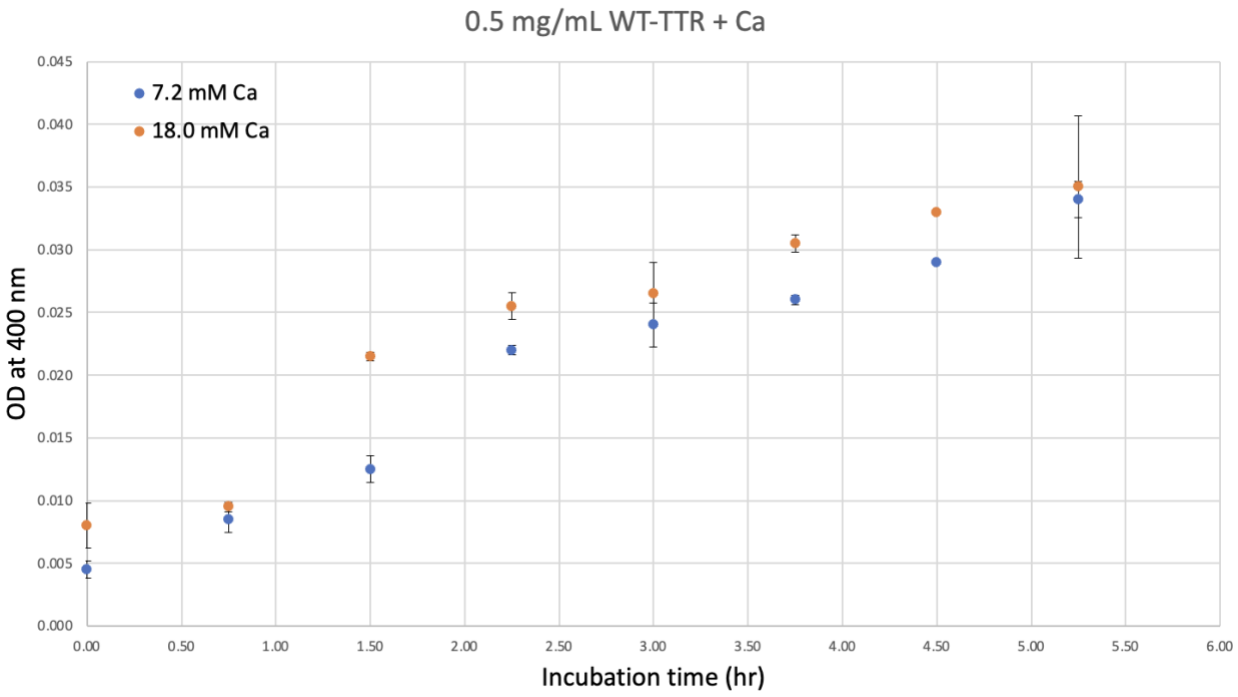

Figure 4.2: Preliminary data of 0.5mg/ mL WT-TTR + Ca with concentrations of 7.2 mM and 18.0 mM of Calcium.

As Calcium was still shown to be effective, the next step was to compare it to the metal ion Zn^{2+}. Samples were prepared for both V30M and WT and were completed in a comparative analysis. As seen in Figures 4.3 and 4.4, V30M was shown to be more effective when combined with the Zn^{2+} ions and had a much faster aggregation period when compared to that of the WT samples. The initial data shows that V30M is consistently more reactive with both metals compared to WT.

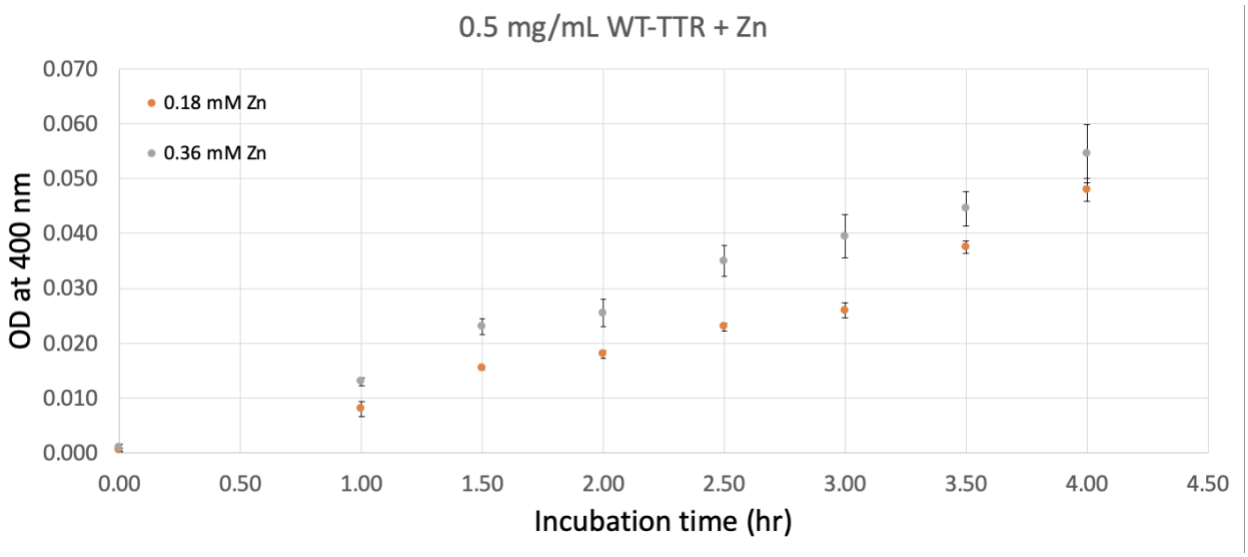

Figure 4.3: Preliminary data of 0.5mg/ mL WT-TTR + Zn with the concentrations of 0.18 mM and 0.36 mM of Zinc.

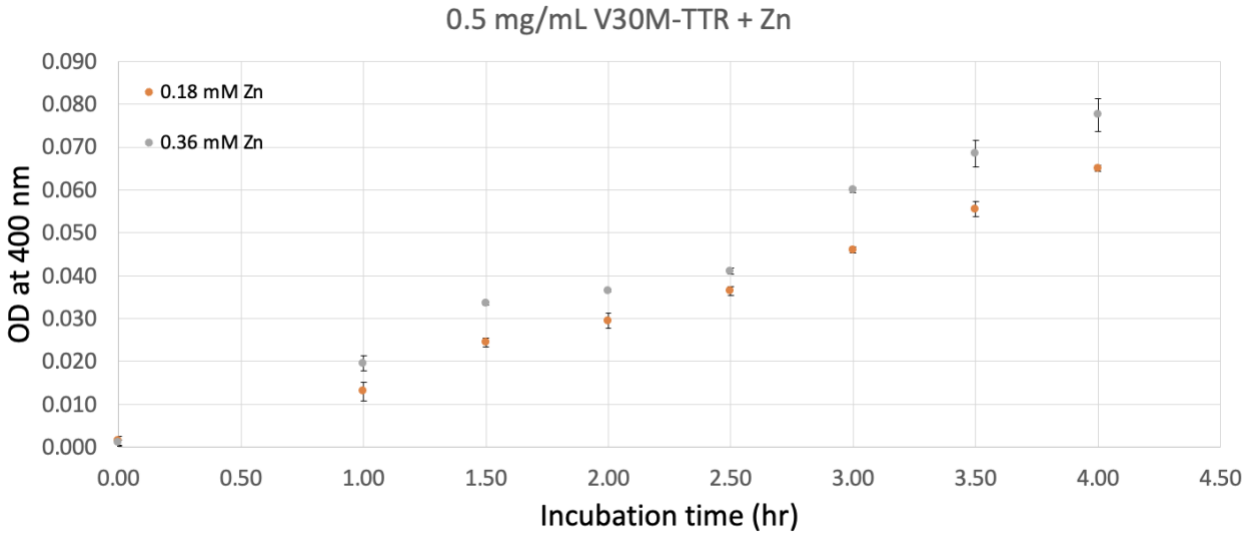

Figure 4.4: Preliminary data of 0.5mg/ mL WT-TTR + Zn with the concentrations of 0.18 mM and 0.36 mM of Zinc.

Between the initial data collection, it is evident that Zn^{2+} is overall more effective compared to Ca^{2+} as it has a higher effective aggregation period for each of the mutations used

during this experiment. There is also a distinguishable difference in the amount of metal present in each sample to be effective. The higher metal presence in each sample also presented a more effective complex in the mutates with the use of Zn^{2+}. This correlation presented that both Ca^{2+} and Zn^{2+} complexes have a consistent effect on the aggregation of the samples at physiological pH. The overall purpose of the preliminary results was to indicate the optimization of the experimental conditions for further investigation the protein and when aggregation was induced.

4.1.2 Final Results

In further experimentation, aggregation kinetics was completed as a comparative analysis with both mutations over a period of time (7 hours) at physiological pH as these conditions are stable in the human body. These results indicated the effects of different amounts of metal ions with protein aggregation properties over a period of time. Figures 4.5 and 4.6 show the correlation of how different variations of Ca^{2+} introduced into V30M and WT affect protein aggregation. As shown the amount of metal solution used in each sample shows a consistent aggregation correlation pattern. The higher concentration has a faster aggregation rate compared to the lower concentration rate. Compared to the initial data collected the data is consistent and shows that the longer the duration of the experiment the results are shown to be consistent. During this comparative analysis of $Ca^{2+,}$ it shows that V30M is more reactive to the metal present than that of the WT which is consistent with the preliminary results.

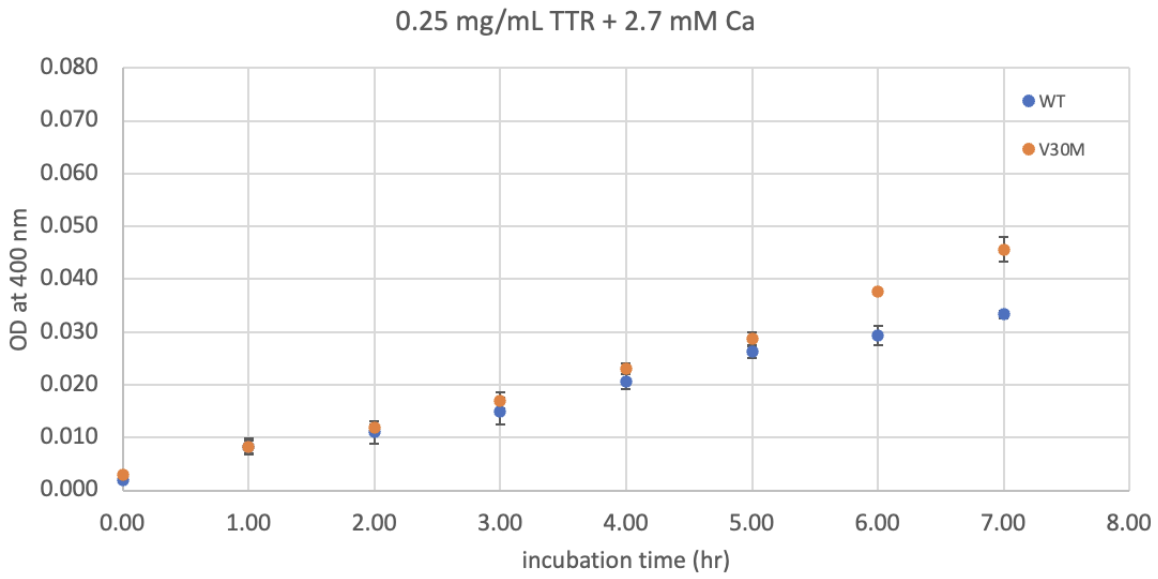

Figure 4.5: Final data collected with a Ca^{2+} concentration of 2.71 mM with a comparison between WT and V30M.

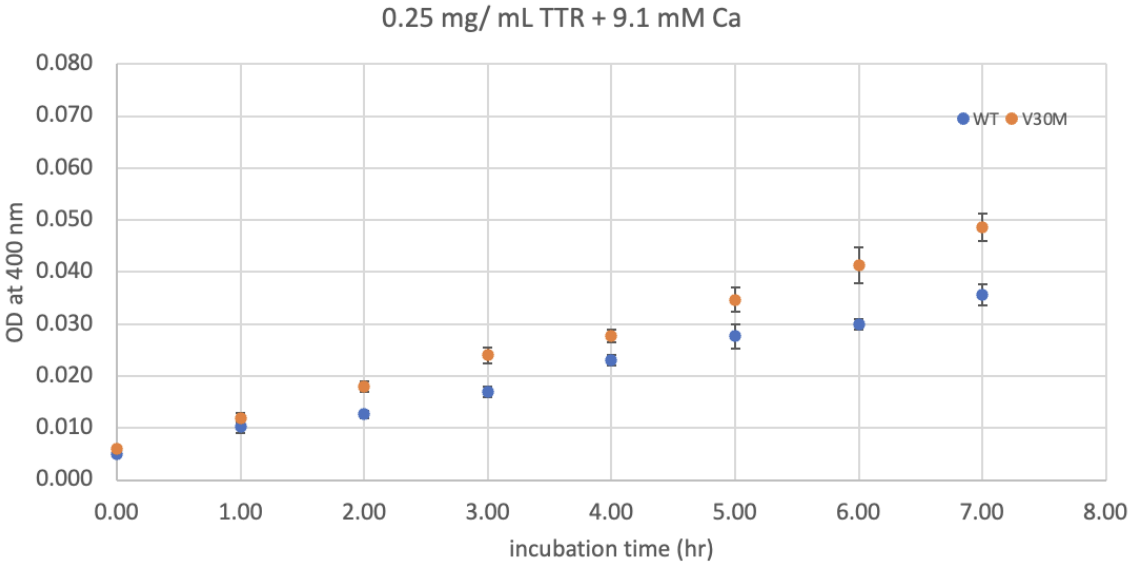

Figure 4.6: Final data collected with a Ca^{2+} concentration of 9.1 mM with a comparison between WT and V30M.

Calcium was shown to be continually effective with each protein. A comparative analysis was also completed for each mutation with the metal ion Zn^{2+}. This comparative analysis was completed for 10 hours. The data collected shown below in Figures 4.7 and 4.8 shows a consistency in the higher the concentration the higher the aggregation. This data is also consistent with the initial data collected with Zn^{2+}.

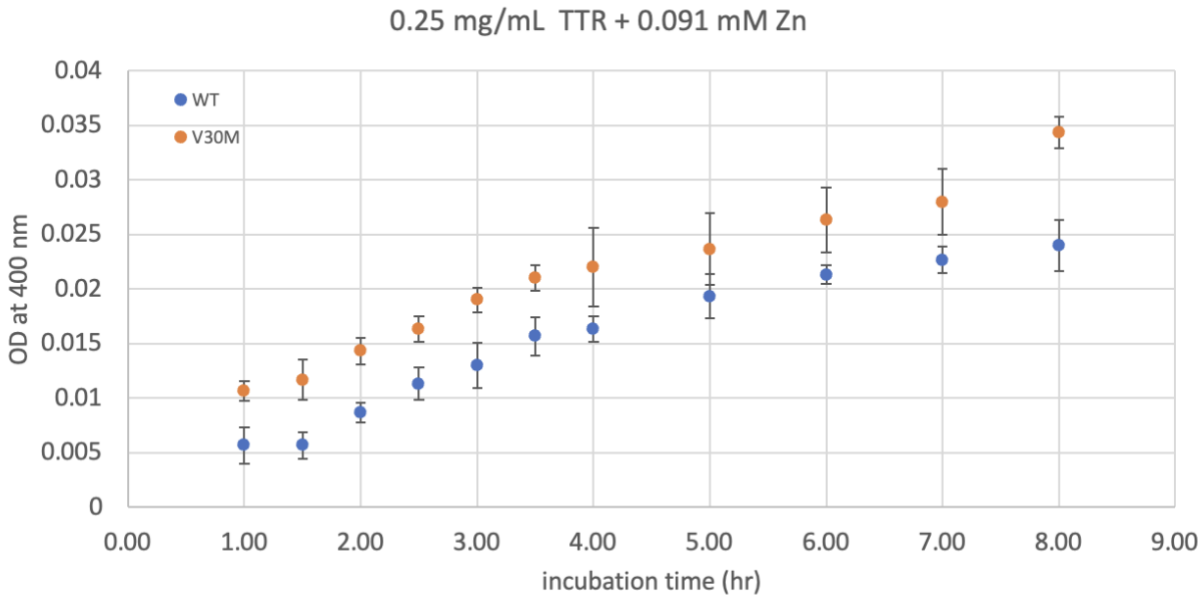

Figure 4.7: Final data collected with a Zn^{2+} concentration of 0.091 mM with a comparison between WT and V30M.

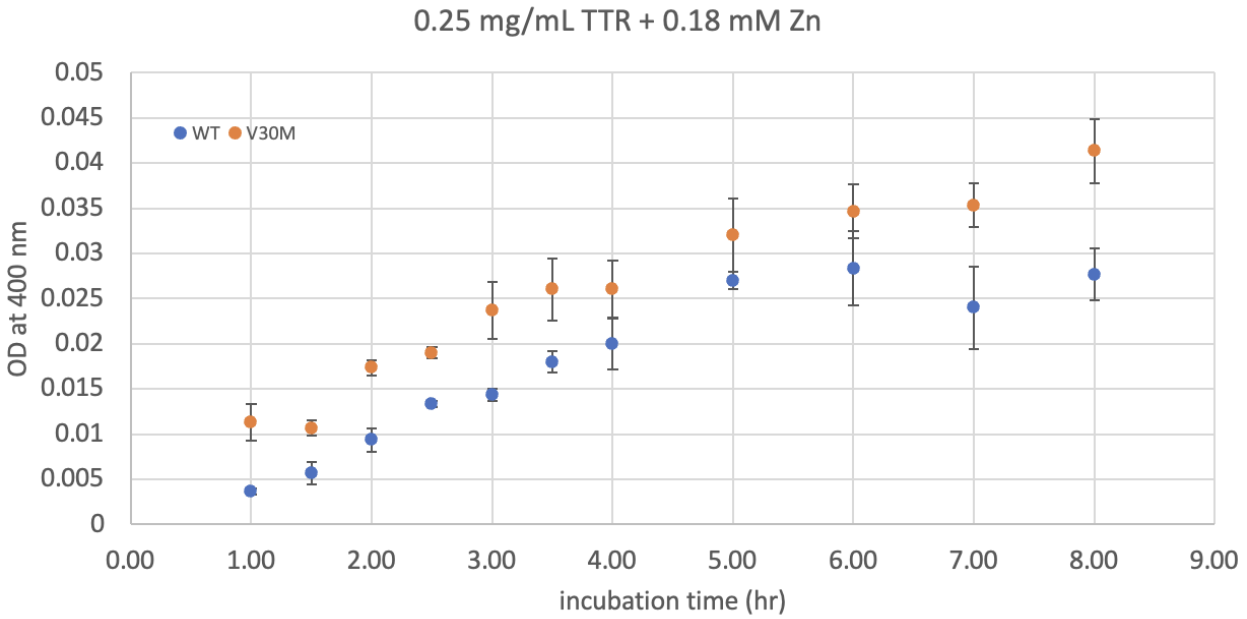

Figure 4.8: Final data collected with a Zn^{2+} concentration of 0.18 mM with a comparison between WT and V30M.

Overall, the Zn^{2+} shows a higher effectiveness comparatively to the Ca^{2+} ions in both comparative analyses. This is consistent with the initial results showing that the data is continuing to be consistent over a longer period of time. The data collected also shows a higher effective aggregation period for each of the proteins used during experimentation with Zn^{2+}. The comparative analysis also shows that the V30M mutation has a higher aggregation rate compared to the WT, which with previous analysis shows to still hold consistent in what is known about each protein. Between both metal solutions used throughout the aggregation kinetics process, it has been observed that the samples are producing aggregates. However, a difference is seen as the higher the concentration the faster aggregates are being produced which shows a spread between the concentrations as the gap becomes wider the more aggregates are being created at a significantly higher rate over time until it becomes stable.

4.2 Circular Dichroism

4.2.1 Preliminary Results

Circular Dichroism raw data was initially collected and placed into a spreadsheet to create graphs to observe the effects the metal binding had on WT. The sample proteins were tested with the native structure and with individual binding of Zn^{2+} and Ca^{2+} to the protein. Below Figure 4.9 shows the initial data collected for WT with each metal-induced and native protein.

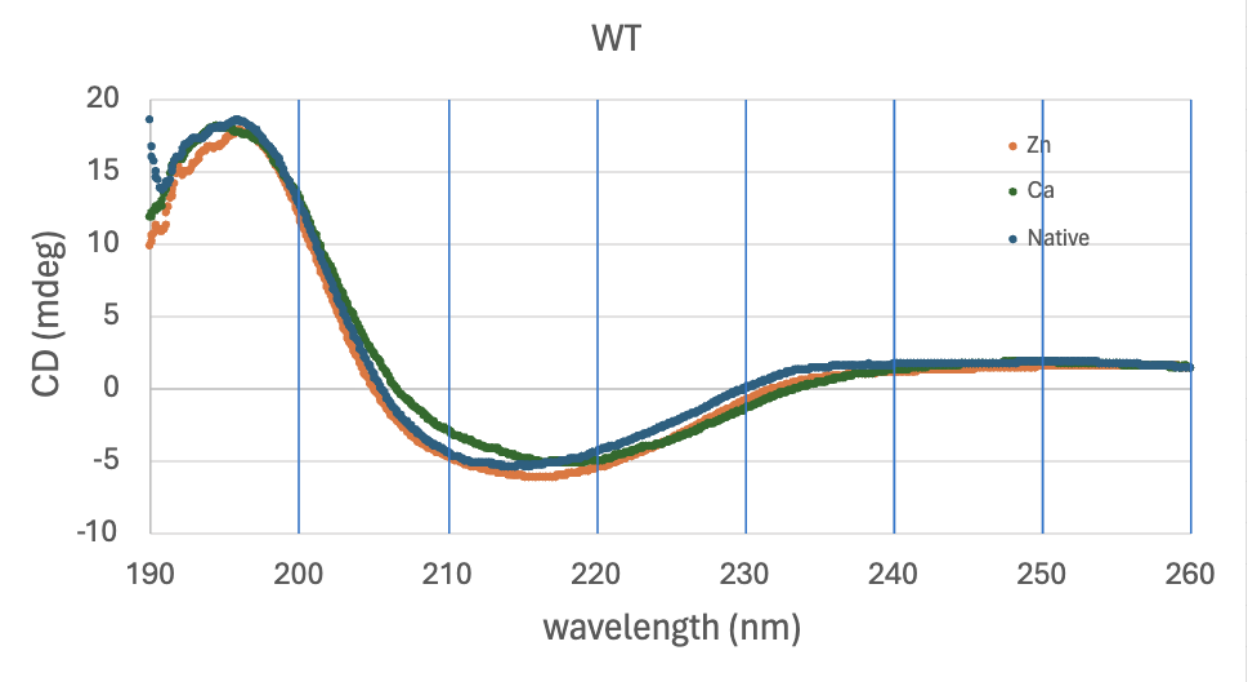

Figure 4.9: Initial CD data collected of WT with Zn^{2+} and Ca^{2+} induced protein in comparison with the native WT protein.

In Figure 4.9, the native protein was used as a baseline to compare the metal binding to the samples, and based on each of the metal samples there is a slight shift in the secondary structure. Though the structure is shifting it is still primarily representing a β-sheet type

secondary structure for native for both Zn^{2+} and Ca^{2+} induced samples. The small shifts are typically for proteins that have a lower binding infinity. These results were helpful in the determination of the effects the metal is having on the protein. The next step was observing the metals being bound with a known mutate V30M and continually analysis of WT. The preliminary results were used to determine the optimizable conditions for further investigation of the secondary structure when interacting with the metal ions.

4.2.2 Final Results

Circular Dichroism raw data was initially collected and placed into a spreadsheet to create graphs to observe the effects the metal binding had on WT and V30M. The sample proteins were tested with the native structure and with individual binding of Zn^{2+} and Ca^{2+} induced with the protein. Below Figure 4.10 shows the data collected for WT with each metal-induced and native protein.

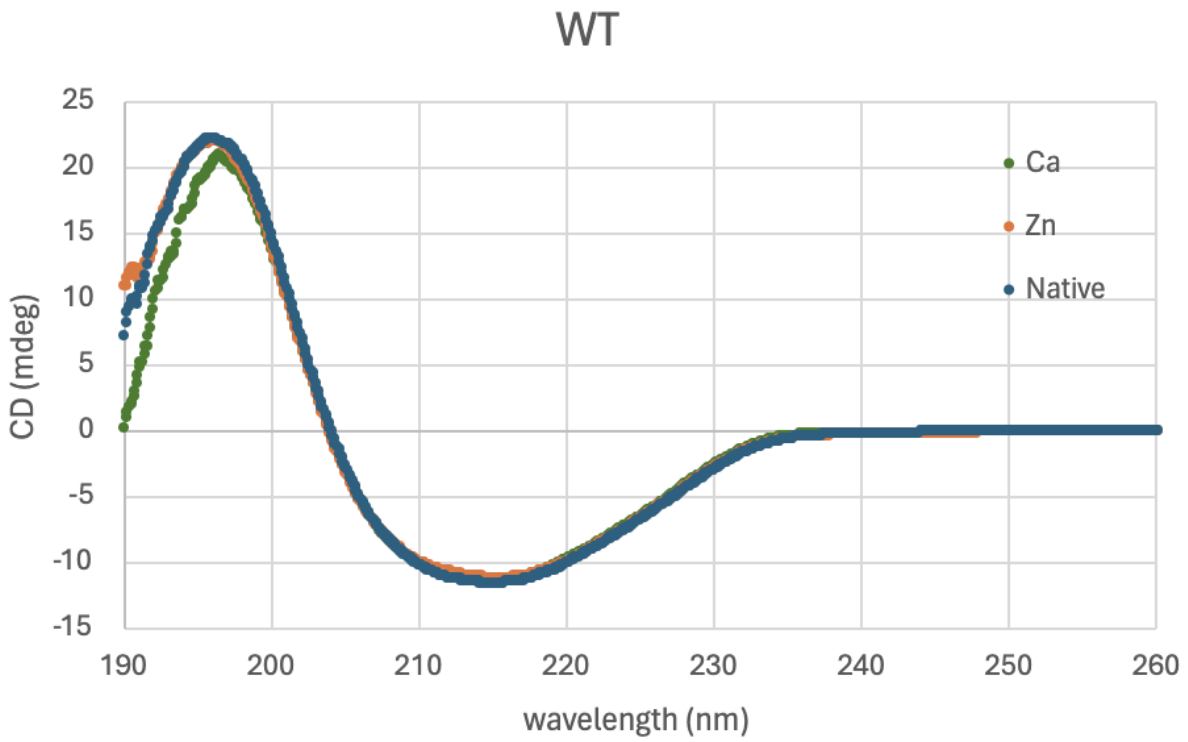

Figure 4.10: Final CD data collected of WT with Zn^{2+} and Ca^{2+} induced protein in comparison with the native WT.

In Figure 4.10, the native protein was used as a baseline to compare the metal-bound samples. Based on the Zn^{2+} and Ca^{2+} bound to the protein show small structural changes which is indicated by the small shifts of each of the metal-induced proteins compared to the native protein. These shifts are consistence with the initial data collected in Figure 4.9 along with the secondary structure of the protein. This information shows that WT changes over an extensive period of time are still small in the structural changes when binding to these specific metals to the protein. V30M was then analyzed with Zn^{2+} compared to the native type below in Figure 4.11.

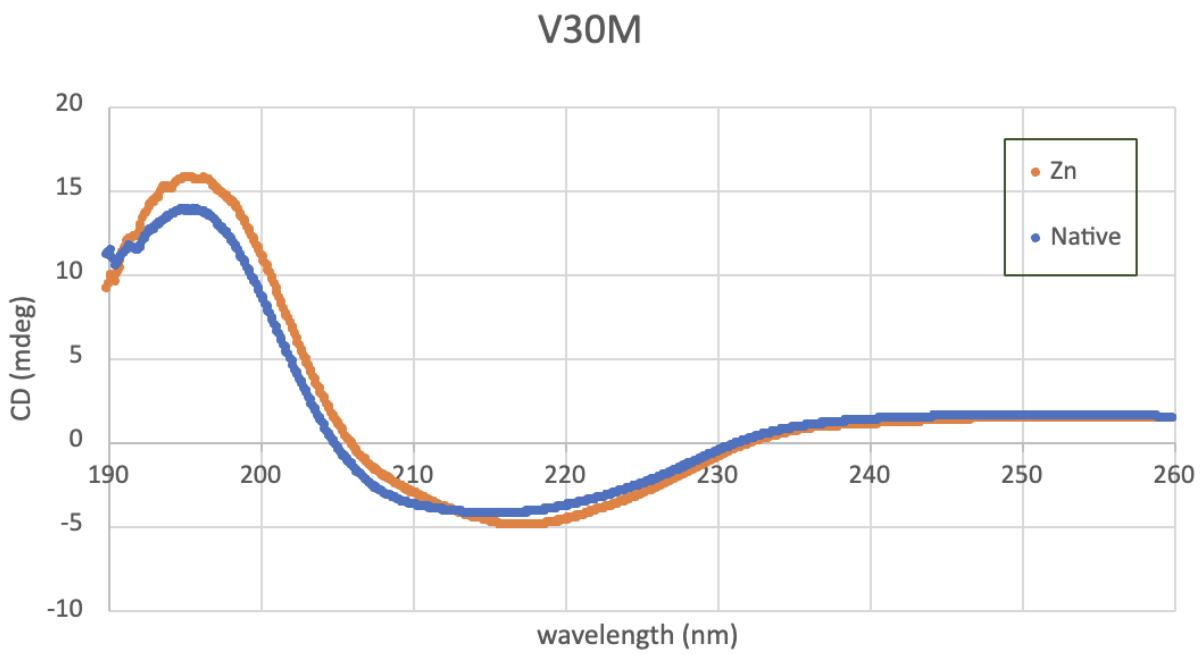

Figure 4.11: Initial CD data collected of V30M with Zn^{2+} induced protein in comparison with the native V30M.

The native sample shown above was used as a baseline for each of the metal samples. The metal-induced sample shows small local changes within the structure which is noticeable due to the shift in the data compared to the native sample. The overall secondary structure represented for each sample is primarily β-sheet. Based on WT and V30M data V30M has a higher shift in Zn^{2+} induced sample, this is expected as WT has a slower aggregation period compared to the mutate V30M.

4.3 Isothermal Titration Calorimeter

4.3.1 Preliminary Results

Isothermal Titration Calorimeter raw data was collected and placed into the data analysis software Nanoanaylze. The information collected from the ITC and data analysis software shows the determination of the measure of heat changes associated with the binding of a metal. The data also is informative in the collection of binding affinity (KD), enthalpy (ΔH), entropy (ΔS), and stoichiometry (N). The preliminary results collected for the protein sample of WT were tested with Zn^{2+} as it has been a more notable metal that interacts with the protein. The data collected is below in Figure 4.12.

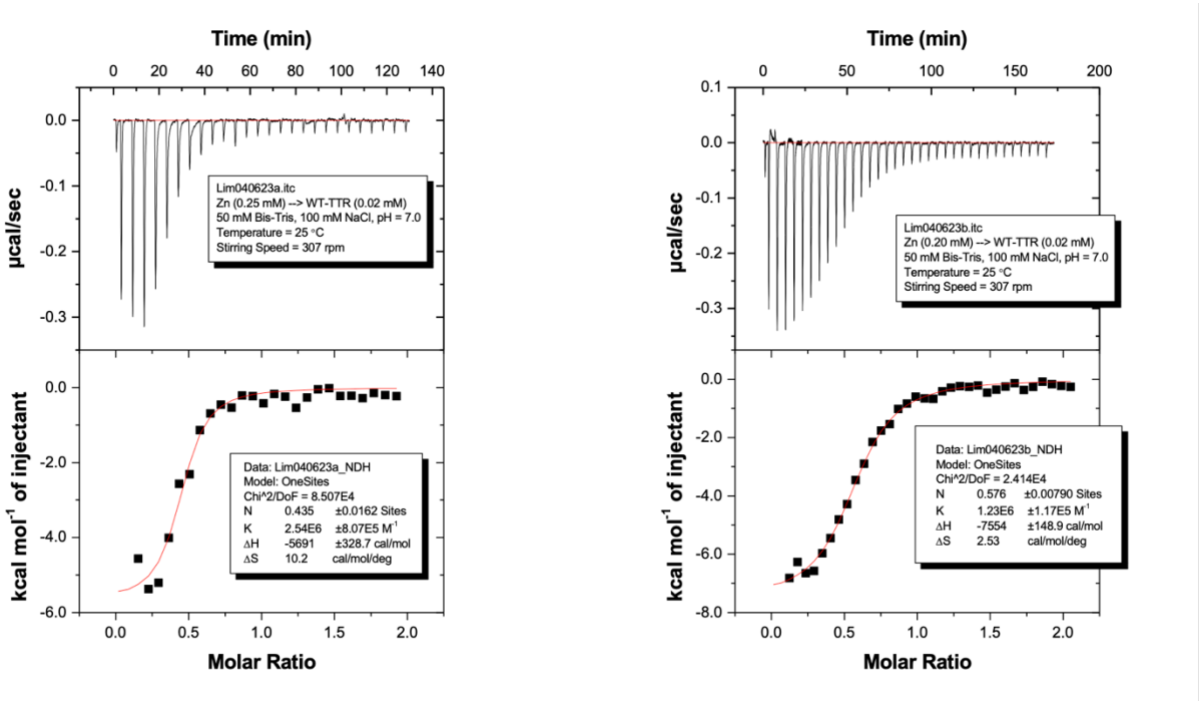

Figure 4.12: Initial ITC data collection of WT with Zn^{2+}.

The figure above shows two exothermic reactions of the Zn^{2+} ions solution being titrated into the WT. The reactions did meet equilibrium which is prominent when conducted ITC. The data

collected showed the enthalpy being typical for an ITC experiment and that the entropy was positive indicating that entropy was allowing the binding event to occur. The binding affinity was determined to be $3.94E^{-7}$ for run a and $8.12E^{-7}$ for run b. This indicates the strength of the interaction being a strong reaction. The stoichiometry value is an indicator of the binding of the metal as shown in the figure above there is half a binding site that is occurring though it is unknown where the binding site is occurring. With an indication of a binding site, further investigation was completed. The preliminary results were used to find the optimal conditions to further investigate the binding of the metal with the protein.

4.3.2 Final Results

ITC raw data was collected and placed into the data analysis software Nanoanaylze. The information collected from the ITC and data analysis software shows the determination of the measure of heat changes associated with the binding of a metal. The results collected for the sample of WT were tested with Zn^{2+} based on confirmed information collected from the preliminary data above. The final data collected for two runs is shown below in Figure 4.13.

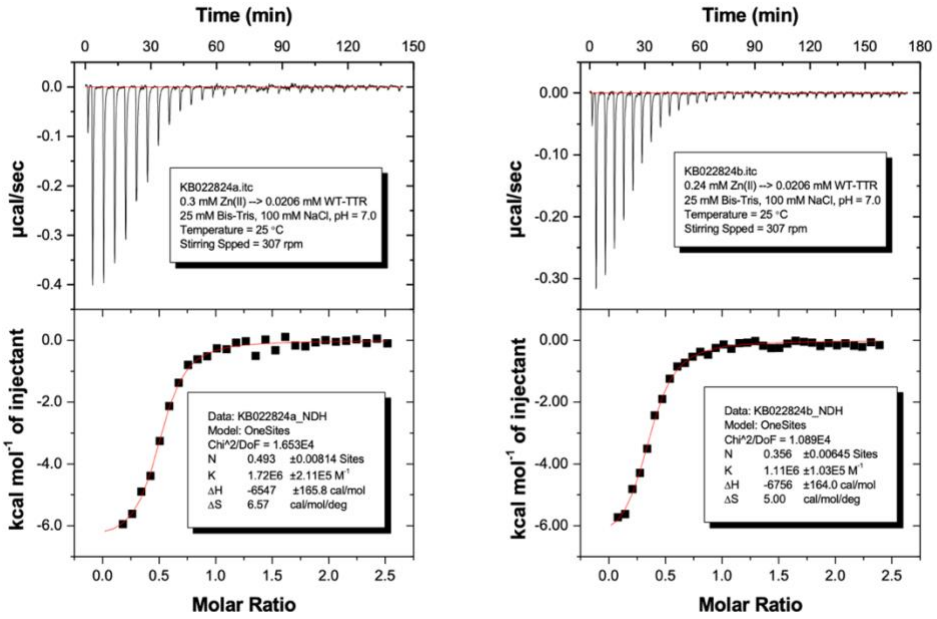

Figure 4.13: Final ITC data collection of WT with Zn^{2+}**.**

The figure above shows the exothermic reactions of the Zn^{2+} ions solution being titrated into the WT for two ITC runs. The data collected showed the enthalpy to be typical for an ITC experiment and that the entropy was positive indicating the binding site was to occur. The binding affinity was determined to be $5.81E^{-7}$ for run a and $9.00E^{-7}$ for run b. The stoichiometry value shown in the figure above there is half a binding site that is occurring. This indicates the preliminary data and the final data to be consistence.

Overall, between the preliminary results and the final results there is an indication of half a binding site occurring; shows a small occurrence of binding as there are sixteen binding sites and twelve known binding sites for the native protein and it is expected that at least half of them would bind to the structure and be indicated through ITC. Along with positive entropy, this indicated that the metal was inducing local conformational fluctuations, which may accelerate

the dissociation of the native tetramer. From the results, future research is needed to further investigate the structural changes and binding information.

Chapter 5

Conclusions and Future Directions

The molecular mechanism of transthyretin of natively folded protein structural transitions to the product of amyloids is intricately complex and little is known about the process. There have been many studies conducted to view the transition from the native folded to the unfolded (full or partial) intermediate states showing the possibility of mutations such as conformational transitions and acceleration of misfolded proteins and aggregation [31,32]. Each of those studies hypothesized that the changes are typically seen during transitions of the protein formation mechanism. The current known mutations of transthyretin show possibilities of metal-inducing protein aggregation, which then produces amyloid fibrils. This study aimed to investigate further how metals such as Zn^{2+} and Ca^{2+} ions impacted the protein and view of induced aggregation as each of these metals is naturally found within the body [20,22]. Each metal plays a different role in the protein mechanism with induced aggregation. It was prominent that each metal has a specific role in the protein mechanism during induced aggregation such as structural changes to the secondary structure and specific metal binding sites.

Upon initial testing of aggregated kinetics, the native protein and mutated protein showed induced aggregation by Zn^{2+} and Ca^{2+} ions at physiological pH. This information indicated that aggregates were being formed and further testing was pursued to indicate structure information on how the metals were affecting the protein. Circular Dichroism testing was completed to indicate any structural changes that the metal ions would have induced. Through further testing, it was shown to have little secondary structural changes to either the native or mutated protein from either metal that was introduced. This indicated local structural changes occurred but had no significant impact on the secondary structure of the protein. This introduced early testing with

the use of Isothermal Titration Calorimetry, where binding affinity and binding sites could be determined, along with the entropy and enthalpy of the metal-protein interaction. This early testing of the native protein with the metal ion Zn^{2+} showed a moderate binding affinity indicating a higher possibility of metal binding to the protein. There was also an indication of the presence of a half-binding site occurring. This further indicated that the metal was binding and proved that the metal was also inducing aggregates of the protein.

The biophysical analyses revealed the metal ion bindings induced local structural/ dynamical changes of the protein, promoting misfolding and aggregation. Based on ITC results there is an indication of a possible bridge binding between the metal and two monomers of the protein. Future studies will aid in the determination of how the metal is binding and if there is a bridging of the metal with monomers. Future studies will also further structural determination of proteins in their native and mutated form with the use CYRO-EM as it shows the protein's structure, which would overall aid in seeing the structure of the different forms of the protein. It would also aid in the determination of the possibility of the metals elongating the fibrils and/ or the formation of either fibrils or amyloids.

The information collected is still very early in understanding how these metals affect the protein in a native and mutated form. With this testing, it was determined that the metals induced aggregates and induced local structural changes to the proteins. This leads to the possibility of forming fibrils, which is significant in the research in aiding in further investigation with comparative analysis of WT and V30M to other mutations such as L55P and V122I as each mutation of the protein has a different impact on the body. Each mutation may also have a different interaction with the metal ions compared to another mutation. Comparative analysis will be imperative in future research in continuing to understand the structural formation and the

metal's interaction with the protein’s structure. The impact of this study further indicates the importance of future research and the importance of determining what aggregates are being formed with WT and V30M. This study may aid in future investigative studies that may aid in determining future treatments for those with hereditary amyloidosis, senile systemic amyloidosis, familial amyloidosis cardiomyopathy, and familial amyloidosis polyneuropathy.

References

(1) Bezerra, F.; Saraiva, M. J.; Almeida, M. R. Modulation of the Mechanisms Driving Transthyretin Amyloidosis. *Front. Mol. Neurosci*. **2020**, *13*, 592644. https://doi.org/10.3389/fnmol.2020.592644

(2) Frederick L. Ruberg, Martha Grogan, Mazen Hanna, Jeffery W. Kelly, Mathew S. Maurer, Transthyretin Amyloid Cardiomyopathy: JACC State-of-the-Art Review, Journal of the American College of Cardiology, Volume 73, Issue 22, 2019, Pages 2872-2891, ISSN 0735-1097, https://doi.org/10.1016/j.jacc.2019.04.003.

(3) Jiang X, Labaudinière R, Buxbaum JN, Monteiro C, Novais M, Coelho T, Kelly JW. A circulating, disease-specific, mechanism-linked biomarker for ATTR polyneuropathy diagnosis and response to therapy prediction. Proc Natl Acad Sci USA. 2021 Mar 2;118(9):e2016072118. doi: 10.1073/pnas.2016072118. PMID: 33597308; PMCID: PMC7936353.

(4) Eisele YS, Monteiro C, Fearns C, Encalada SE, Wiseman RL, Powers ET, Kelly JW. Targeting protein aggregation for the treatment of degenerative diseases. Nat Rev Drug Discov. 2015 Nov;14(11):759-80. doi: 10.1038/nrd4593. Epub 2015 Sep 4. PMID: 26338154; PMCID: PMC4628595.

(5) Ciccone, L. (2021, April 22). Effect of Metals in Transthyretin. In Encyclopedia. https://encyclopedia.pub/entry/8900

(6) LaPelusa A, Kaushik R. Physiology, Proteins. [Updated 2022 Nov 14]. In: StatPearls [Internet]. Treasure Island (FL): StatPearls Publishing; 2024 Jan-. Available from: https://www.ncbi.nlm.nih.gov/books/NBK555990/

(7) Moreno-Gonzalez I, Soto C. Misfolded protein aggregates: mechanisms, structures and potential for disease transmission. Semin Cell Dev Biol. 2011 Jul;22(5):482-7. doi: 10.1016/j.semcdb.2011.04.002. Epub 2011 May 5. PMID: 21571086; PMCID: PMC3175247.

(8) L. Breydo, V.N. Uversky
Structural, morphological, and functional diversity of amyloid oligomers
FEBS Lett., 589 (2015), pp. 2640-2648

(9) Rambaran RN, Serpell LC. Amyloid fibrils: abnormal protein assembly. Prion. 2008 Jul-Sep;2(3):112-7. doi: 10.4161/pri.2.3.7488. Epub 2008 Jul 20. PMID: 19158505; PMCID: PMC2634529

(10) R. Wetzel, Amyloid, W.J. Lennarz, M.D. Lane (Eds.), Encyclopedia of Biological Chemistry (second ed.), Academic Press, Waltham (2013), pp. 100-104, 10.1016/B978-0-12-378630-2.00167-5

(11) Ajmal MR. Protein Misfolding and Aggregation in Proteinopathies: Causes, Mechanism and Cellular Response. Diseases. 2023 Feb 9;11(1):30. doi: 10.3390/diseases11010030. PMID: 36810544; PMCID: PMC9944956.

(12) Bustamante JG, Zaidi SRH. Amyloidosis. [Updated 2023 Jul 31]. In: StatPearls [Internet]. Treasure Island (FL): StatPearls Publishing; 2024 Jan-. Available from: https://www.ncbi.nlm.nih.gov/books/NBK470285/

(13) Guan J, Mishra S, Falk RH, Liao R. Current perspectives on cardiac amyloidosis. Am J Physiol Heart Circ Physiol. 2012 Feb 1;302(3):H544-52. doi: 10.1152/ajpheart.00815.2011. Epub 2011 Nov 4. PMID: 22058156; PMCID: PMC3353775.

(14) Baker KR, Rice L. The amyloidoses: clinical features, diagnosis and treatment. Methodist Debakey Cardiovasc J. 2012 Jul-Sep;8(3):3-7. doi: 10.14797/mdcj-8-3-3. PMID: 23227278; PMCID: PMC3487569.

(15) Ruberg FL, Berk JL. Transthyretin (TTR) cardiac amyloidosis. Circulation. 2012 Sep 4;126(10):1286-300. doi: 10.1161/CIRCULATIONAHA.111.078915. PMID: 22949539; PMCID: PMC3501197.

(16) Adams D. Recent advances in the treatment of familial amyloid polyneuropathy. Ther Adv Neurol Disord. 2013 Mar;6(2):129-39. doi: 10.1177/1756285612470192. PMID: 23483184; PMCID: PMC3582309.

(17) Ruberg FL, Grogan M, Hanna M, Kelly JW, Maurer MS. Transthyretin Amyloid Cardiomyopathy: JACC State-of-the-Art Review. J Am Coll Cardiol. 2019 Jun 11;73(22):2872-2891. doi: 10.1016/j.jacc.2019.04.003. PMID: 31171094; PMCID: PMC6724183.

(18) I. Katona, J. Weis, Diseases of the peripheral nerves,Handb. Clin. Neurol., 145 (2017), pp. 453-474

(19) Plante-Bordeneuve V, Said G. Familial amyloid polyneuropathy. *Lancet Neurol.* 2011;10:1086–1097.

(20) Palm R, Hallmans GZinc concentrations in the cerebrospinal fluid of normal adults and patients with neurological diseases.*Journal of Neurology, Neurosurgery & Psychiatry* 1982;**45:**685-690.

(21) Goldstein DA. Serum Calcium. In: Walker HK, Hall WD, Hurst JW, editors. Clinical Methods: The History, Physical, and Laboratory Examinations. 3rd edition. Boston:

Butterworths; 1990. Chapter 143. Available from:

https://www.ncbi.nlm.nih.gov/books/NBK250/

(22) Forsberg M, Seth H, Björefeldt A, Lyckenvik T, Andersson M, Wasling P, Zetterberg H, Hanse E. Ionized calcium in human cerebrospinal fluid and its influence on intrinsic and synaptic excitability of hippocampal pyramidal neurons in the rat. J Neurochem. 2019 May;149(4):452-470. doi: 10.1111/jnc.14693. Epub 2019 Apr 9. PMID: 30851210.

(23) The Physiological, Biochemical, and Molecular Roles of Zinc Transporters in Zinc Homeostasis and Metabolism, Taiho Kambe, Tokuji Tsuji, Ayako Hashimoto, and Naoya Itsumura, Physiological Reviews 2015 95:3, 749-784

(24) Guo X, Liu Z, Zheng Y, Li Y, Li L, Liu H, Chen Z, Wu L. Review on the Structures and Activities of Transthyretin Amyloidogenesis Inhibitors. Drug Des Devel Ther. 2020 Mar 10;14:1057-1081. doi: 10.2147/DDDT.S237252. PMID: 32210536; PMCID: PMC7071892.

(25) Zhou, S.; Cheng, J.; Yang, T.; Ma, M.; Zhang, W.; Yuan, S.; Lo, G.V.; Dou, Y. Exploration of the Misfolding Mechanism of Transthyretin Monomer: Insights from Hybrid-Resolution Simulations and Markov State Model Analysis. *Biomolecules* **2019**, *9*, 889.

(26) Schonhoft JD, Monteiro C, Plate L, Eisele YS, Kelly JM, Boland D, Parker CG, Cravatt BF, Teruya S, Helmke S, Maurer M, Berk J, Sekijima Y, Novais M, Coelho T, Powers ET, Kelly JW. Peptide probes detect misfolded transthyretin oligomers in plasma of hereditary amyloidosis patients. Sci Transl Med. 2017 Sep 13;9(407):eaam7621. doi: 10.1126/scitranslmed.aam7621. PMID: 28904227; PMCID: PMC5628019.

(27) Novel Zn2+-binding Sites in Human Transthyretin, Palmieri, Leonardo de C. et al., Journal of Biological Chemistry, Volume 285, Issue 41, 31731 - 31741

(28) Palmieri Lde C, Lima LM, Freire JB, Bleicher L, Polikarpov I, Almeida FC, Foguel D. Novel Zn2+-binding sites in human transthyretin: implications for amyloidogenesis and retinol-binding protein recognition. J Biol Chem. 2010 Oct 8;285(41):31731-41. doi: 10.1074/jbc.M110.157206. Epub 2010 Jul 20. PMID: 20659897; PMCID: PMC2951245.

(29) Forsberg, M., Seth, H., Björefeldt, A., Lyckenvik, T., Andersson, M., Wasling, P., Zetterberg, H. and Hanse, E. (2019), Ionized calcium in human cerebrospinal fluid and its influence on intrinsic and synaptic excitability of hippocampal pyramidal neurons in the rat. J. Neurochem., 149: 452-470. https://doi.org/10.1111/jnc.14693

(30) Cantarutti C, Mimmi MC, Verona G, Mandaliti W, Taylor GW, Mangione PP, Giorgetti S, Bellotti V, Corazza A. Calcium Binds to Transthyretin with Low Affinity. Biomolecules. 2022 Aug 2;12(8):1066. doi: 10.3390/biom12081066. PMID: 36008960; PMCID: PMC9406000.

(31) Dasari AKR, Yi S, Coats MF, Wi S, Lim KH. Toxic Misfolded Transthyretin Oligomers with Different Molecular Conformations Formed through Distinct Oligomerization Pathways. Biochemistry. 2022 Nov 1;61(21):2358-2365. doi: 10.1021/acs.biochem.2c00390. Epub 2022 Oct 11. PMID: 36219173; PMCID: PMC9665167.

(32) Dasari, A.K.R., Hughes, R.M., Wi, S. *et al.* Transthyretin Aggregation Pathway toward the Formation of Distinct Cytotoxic Oligomers. *Sci Rep* 9, 33 (2019). https://doi.org/10.1038/s41598-018-37230-1

(33) Bateman DA, Tycko R, Wickner RB. Experimentally derived structural constraints for amyloid fibrils of wild-type transthyretin. Biophys J. 2011 Nov 16;101(10):2485-92. doi: 10.1016/j.bpj.2011.10.009. Epub 2011 Nov 15. PMID: 22098747; PMCID: PMC3218328.